Tellus (1985), *37A*, 460–477, Polar Low Special Issue

A numerical study of the development mechanisms of polar lows

By JOSEPH M. SARDIE[1] and THOMAS T. WARNER, *The Pennsylvania State University, Department of Meteorology, University Park, PA 16802, USA*

(Manuscript received October 15, 1984; in final form April 27, 1985)

ABSTRACT

Two well-documented polar lows, one occurring in the Atlantic Ocean and the other in the Pacific Ocean, are modeled *numerically*. These numerical results are compared with our analytic results in order to determine how the effects of nonlinearity and more complete physics may modify our tentative conclusions. The numerical model used in this study is The Pennsylvania State University/National Center for Atmospheric Research (PSU/NCAR), three-dimensional (3-D) primitive equation mesoscale model with a high-resolution planetary boundary-layer parameterization and moist physics. A prediction equation for ground temperature takes into account the existence of variable surface parameters such as albedo, emissivity, thermal inertia, roughness and moisture availability.

The Atlantic polar low developed in a shallow but intense baroclinic zone in the Denmark Strait region during the first 24 h of the forecast period. Sensitivity studies with the 3-D model revealed that the baroclinity was sufficient to allow realistic development while the polar low was in the vicinity of this baroclinic zone. However, both convective and non-convective latent heating and the surface fluxes of sensible and latent heat were necessary for the simulation of observed development after this polar low departed from this baroclinic zone and entered the Norwegian Sea. The fact that convective and non-convective latent heating were both essential for simulating the observed development of the Atlantic polar low is consistent with previous analytic-model results. Like the Atlantic polar low, the Pacific polar low developed in an intense baroclinic zone, but this baroclinic zone was deep. Sensitivity studies revealed that baroclinity in conjunction with only non-convective latent heating, overdeveloped the polar low, unlike the analytic results. It was only through the use of the convective parameterization and the convective heating profile that correct development of the simulated Pacific polar low resulted. Surface fluxes played little role in this development. Thus, moist baroclinity and CISK (conditional instability of the second kind) were both important to the observed development of both the Atlantic and Pacific polar lows.

1. Introduction

Based on a radar study, Harrold and Browning (1969) concluded that the Atlantic polar low is purely baroclinic in origin rather than resulting from some thermal instability process, as thought previously (also see Mansfield, 1974; Duncan, 1977). Rasmussen (1977, 1979, 1981) challenged this new theory and proposed that polar lows forming in the Atlantic Ocean were purely CISK-driven. Reed (1979) and Mullen (1979) investigated polar lows in the Pacific Ocean and proposed baroclinity with CISK as the primary forcing and barotropic instability as the secondary forcing. Also, Økland (1977) has shown that the oceanic sensible heat flux plays an important role in the development of Atlantic polar lows. Using an analytic model of polar lows, Sardie and Warner (1983) found that moist baroclinic processes alone may explain the origin of Pacific polar lows, while both moist baroclinity and CISK seem to be essential in the genesis of Atlantic polar lows. This

[1] Present affiliation: Australian Numerical Meteorology Research Centre, P.O. Box 5089AA, Melbourne, Victoria, 3001, Australia.

hypothesis is being further investigated by using the PSU/NCAR three-dimensional (3-D) model to determine how nonlinear affects and more complete physics may modify these tentative conclusions.

Two cases were chosen for study—one in the Atlantic Ocean and the other in the Pacific Ocean. The specific cases were chosen because they appeared to be representative of Atlantic polar lows, as described by Forbes and Lottes (1982) and Pacific polar lows, as described by Reed (1979) and Mullen (1979). The Atlantic polar low developed in the vicinity of Iceland and Greenland and has been documented by Rasmussen (1981). The Pacific polar low originated in the northern Pacific, southwest of the Aleutians, and has been documented by Locatelli et al. (1982).

Section 2 discusses the numerical model employed in this study; Section 3 briefly illustrates the synoptic situations for both the Atlantic and Pacific cases. Section 4 discusses the design of the numerical experiments, while Section 5 presents the results. Detailed discussion and interpretation of the results are reserved until Section 6. Section 7 compares the numerical results to the analytic results of Sardie and Warner (1983).

2. The numerical model

2.1. The fundamentals

The model used in this study is the PSU/NCAR three-dimensional primitive equation model described in Anthes and Warner (1978). A high resolution planetary boundary-layer parameterization, described by Zhang and Anthes (1982), has been used. Also, the Anthes/Kuo (Anthes, 1977) scheme for convective parameterization employs a modified heating profile calculated using the Fritsch/Chappell (1980) cloud model. A second heating profile, calculated using Anthes (1977) cloud model, is used for comparison. The prediction equation for the ground temperature takes into account variable surface parameters such as albedo, emissivity, thermal inertia, roughness and moisture availability.

The vertical coordinate of the model is σ where $\sigma = (P - P_t)/(P_* - P_t)$, P_t is the pressure at the top of the model and P_* is the surface pressure. The sigma values that bound the model calculation levels used for the Atlantic and Pacific domains are: 0.0, 0.20, 0.30, 0.40, 0.50, 0.60, 0.70, 0.80, 0.85, 0.90, 0.95, 0.998 and 1.00. In the Atlantic case, the grid spacing is 80 km with a (33, 41) domain size and a time step of 150 s. In the Pacific case, the grid spacing is 90 km with a (37, 61 domain size and a time step of 180 s.

2.2. Convection

The vertical heating profiles were obtained from the Fritsch/Chappell (1980) and Anthes (1977) cloud models. The formulation of the Fritsch/Chappell cloud model is based upon the concept that a knowledge of the buoyant energy available to a parcel, in combination with an estimate of the period of time required for the convection to remove that energy, can be used to regulate the amount of convection in a mesoscale numerical model. The formulation of the Anthes (1977) cloud model is based upon the vertical equation of motion and assumes that an updraft is affected by buoyancy, friction and the downward drag of liquid water. The cloud physics follows the simple formulation of Kessler (1965). Soundings of temperature and dewpoint that are representative of the Atlantic and Pacific polar lows were used to obtain heating profiles from the Fritsch/Chappell and Anthes cloud models and these profiles are shown in Fig. 1.

2.3. Sources of data

The data used in the analyses presented in the next section were obtained from three sources. The United States (US) National Meteorological Center's (NMC) operational analysis, defined on the northern hemisphere octagonal (47 × 51) grid, provided winds and temperatures at all standard levels (1000 mb, 850 mb, 700 mb, 500 mb, 400 mb, 300 mb, 250 mb, 200 mb, 150 mb, and 100 mb), relative humidity at three levels and mean sea-level (MSL) pressure. Also, a 63 × 63 grid of U.S. Navy data provided ground temperatures and sea-surface temperatures. Lastly, surface observations provided by the Royal Netherland Meteorological Institute were plotted and used to subjectively analyze MSL pressure charts for the Atlantic case. Data were interpolated from the NMC grid to the Atlantic and Pacific model grids at standard pressure levels using a 16-point Bessel function. Data were then vertically interpolated to pressure levels at 600, 750, 800, 900 and 950 mb. These fields were then enhanced with standard rawinsonde observations. A successive scan

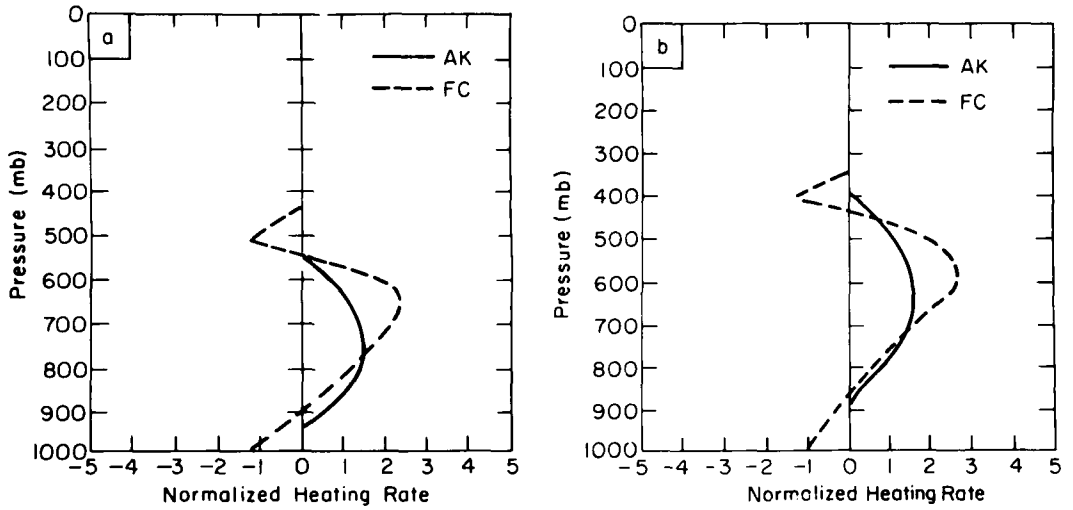

Fig. 1. The normalized heating rate profiles from the Fritsch/Chappell (FC) and Anthes (AK) cloud models, for the Atlantic polar low (a) and for the Pacific polar low (b).

technique, using a hierarchy of isotropic and anisotropic weighting functions, was used for the objective analyses. This method is described in detail in Benjamin and Seaman (1985).

3. The synoptic situations

This section is devoted to a discussion of the meteorological analyses of the two cases. Subsection 3.1 discusses the Atlantic case and Subsection 3.2 the Pacific case. In order to facilitate the description and interpretation of the model results, Table 1 defines model elapsed time as a function of synoptic (or real) time. Times used in the text and the figures are *model elapsed time.*

Table 1. *Model elapsed time as a function of synoptic time*

Atlantic case	
Model elapsed time	Synoptic time
00 h	1200 GMT 23 November 1978
12 h	0000 GMT 24 November 1978
24 h	1200 GMT 24 November 1978
36 h	0000 GMT 25 November 1978
48 h	1200 GMT 25 November 1978
Pacific case	
Model elapsed time	Synoptic time
00 h	0000 GMT 14 December 1977
12 h	1200 GMT 14 December 1977
24 h	0000 GMT 15 December 1977
36 h	1200 GMT 15 December 1977

3.1. The Atlantic case

Fig. 2 shows the MSL pressure analyses at 00 h, 24 h and 48 h. The polar low with a central pressure of 995 mb is initially an extension of a trough extending southwestward from an occluded low near Spitzbergen (not shown). During the next 24 h, it crosses Iceland, and fills to 1001 mb. It is positioned just south of Iceland. In the next 12 h, the low continues to fill to 1004 mb and then deepens to 1003 mb during the final 12 h.

Fig. 3 shows the ground temperature and the sea–surface temperature (SST) analysis at 00 h. A strong temperature gradient exists between Greenland and the waters of the Denmark Strait. This sharp contrast is due to the proximity of the ice-covered land of Greenland, the ice-covered waters along the shores of Greenland and the relatively warm waters of the Gulf Stream in the Denmark Strait. The topography of Greenland also plays a rôle in accentuating this temperature gradient between land and sea. Because this surface gradient is a semipermanent feature in this region at this time of the year, its effects permeate the lower layers of the troposphere. Thus, this atmospheric baroclinic zone is also a semipermanent zone along the Greenland coast during this time of the year,

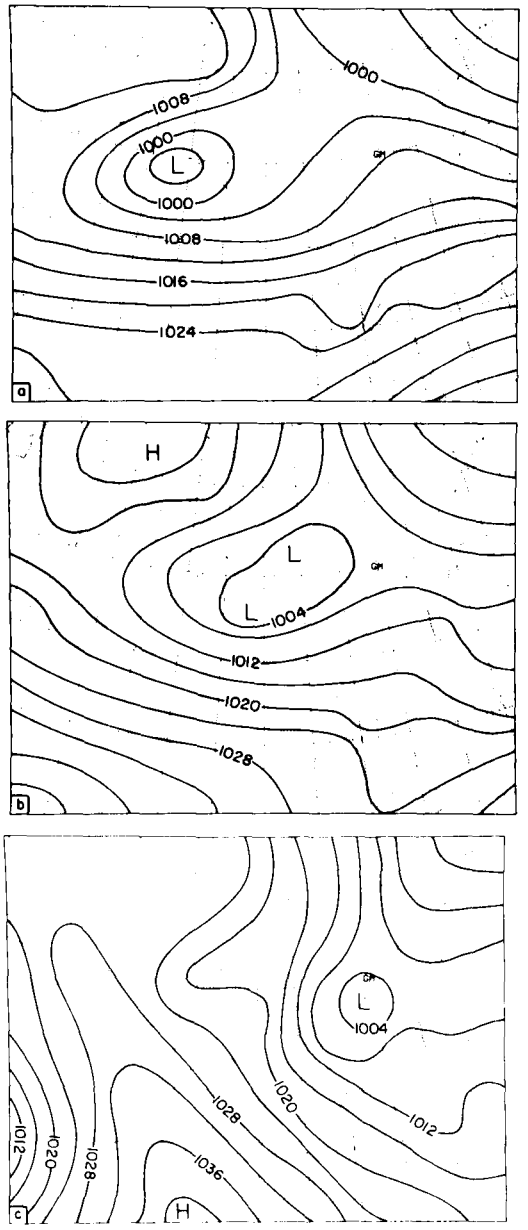

Fig. 2. Analysis of observed MSL pressure (mb) for the Atlantic domain at 1200 GMT 23 November 1978 (00 h) (a), at 1200 GMT 24 November 1978 (24 h) (b), and 1200 GMT 25 November 1978 (48 h) (c).

and is a source of available potential energy (APE). Rasmussen (1981) states that this shallow baroclinic zone plays a dynamic role in the development of this polar low. The SST analysis

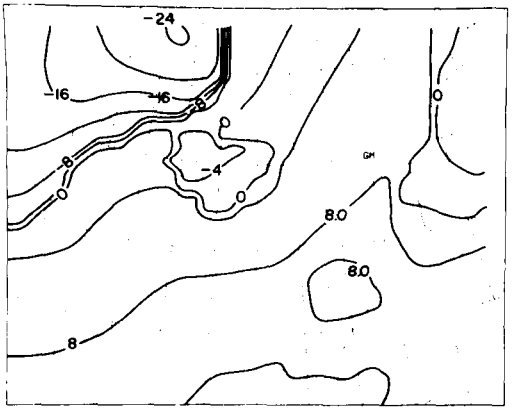

Fig. 3. Analysis of observed ground temperature and sea-surface temperature (C) for the Atlantic domain at 1200 GMT 23 November 1978 (00 h).

also shows a tongue of warm water extending northward from the Atlantic Ocean into the Norwegian Sea. The role of this tongue of high SST in allowing substantial sensible heat and moisture fluxes from the ocean to the developing polar low is discussed in Section 6.

3.2. The Pacific case

Fig. 4 shows the MSL pressure analyses at 00 h, 24 h and 36 h. A large trough initially extends southwestward from the Gulf of Alaska low (with a central MSL pressure of 960 mb) to the genesis area of the polar low. (This Gulf of Alaska low will be referred to here as the Gulf low.) There is a ridge of high pressure extending from the southern North Pacific over California and a trough of low pressure extending from the Gulf low eastward toward Canada. During the first 12-h period, the Gulf low deepens to 953 mb, while a small but organized convective cloud field moves around the Gulf low to the south, coincident with a well-defined, deepening surface trough. During the second 12-h period, the polar trough progressively moves eastward, deepening from 994 mb to 990 mb. The central MSL pressure of the Gulf low is now 954 mb. During the third 12-h period of the 36-h simulation, the polar trough develops a pressure minimum (polar low) and deepens to 986 mb, while the Gulf low fills to 967 mb.

Fig. 5 shows the ground temperature and the SST analysis at 00 h. Note that there exists a small tongue of warm water along the west coast of the

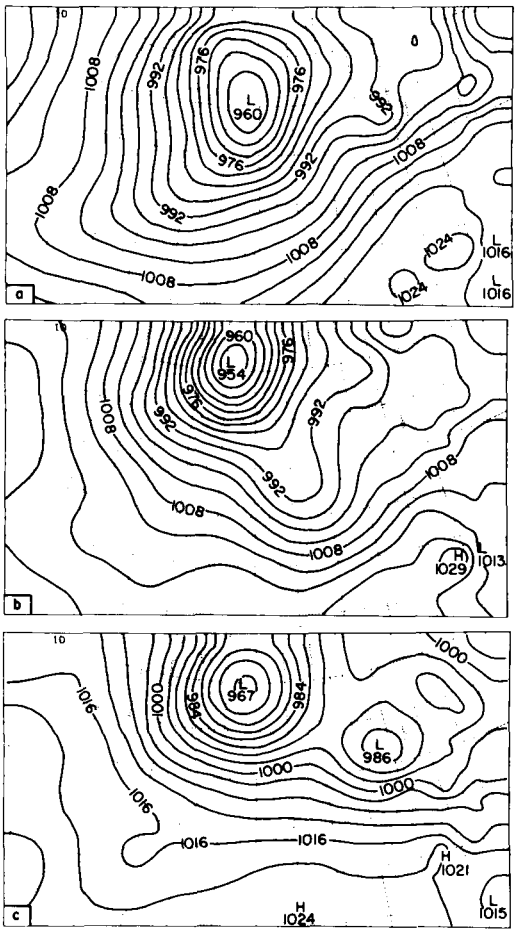

Fig. 4. Analysis of observed MSL pressure (mb) for the Pacific domain at 0000 GMT 14 December 1977 (00 h) (a), 0000 GMT 15 December 1977 (24 h) (b), and 1200 GMT 15 December 1977 (36 h) (c).

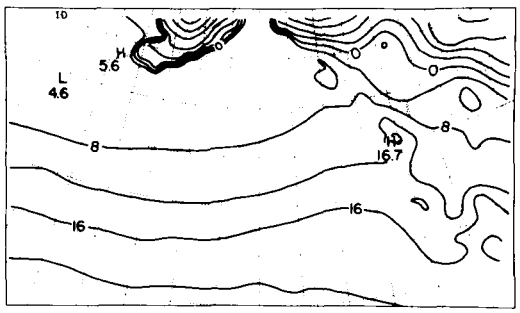

Fig. 5. Analysis of observed ground temperature (C) and sea-surface temperature (C) for the Pacific domain at 0000 GMT 14 December 1977 (00 h).

U.S. The role of this tongue of high SST, in the evolution of the polar low, is discussed in Section 6.

4. Design of the experiments

In order to investigate the dynamic processes associated with the genesis of Atlantic and Pacific polar lows, a series of numerical experiments was designed. This series of experiments is summarized in Table 2. A code for each experiment is shown in the table and will subsequently be used in the text and the figure captions. The experimental design was chosen to be as consistent as possible with the design of the analytical experiments of Sardie and Warner (1983), so that a comparison can be made in Section 7 between the analytical and the numerical results. The experimental design for each case consists of performing two control simulations which contain complete physics and three sensitivity experiments with modified physics,

Table 2. *Design of Atlantic and Pacific experiments*

Code	Purpose of experiment	Description of experiment
CFC	control forecast	complete model physics: convective and non-convective precipitation, with a convective heating profile from Fritsch/Chappell (1980) cloud model
CAK	control forecast	complete model physics: convective and non-convective precipitation, with a convective heating profile from Anthes (1977) cloud model
DRY	sensitivity study	modified physics: no convective parameterization scheme and no non-convective precipitation; surface fluxes of heat were allowed
NCO	sensitivity study	modified physics: no convective parameterization scheme; non-convective precipitation and surface fluxes of heat and moisture were allowed
NFL	sensitivity study	modified physics: no surface sensible and latent heat fluxes; complete moisture physics otherwise

and comparing the results to gain insight into the prevailing dynamic processes.

Because there is uncertainty concerning the appropriate structure of a CISK-type heating profile (Kuo, 1965, 1971, 1974; Anthes, 1977; Fritsch and Chappell, 1980; Ooyama, 1982) the control experiment is run twice for each case, using two different convective heating profiles. The CFC simulation uses a convective heating profile obtained from the Fritsch/Chappell cloud model, while the CAK simulation uses a convective heating profile obtained from the Anthes cloud model. The control simulation conditions correspond to the BCM (moist baroclinic)/CISK mode conditions defined in the analytic study by Sardie and Warner (1983).

The dynamic importance of latent heating is determined by allowing no feedback of latent heat release in the thermodynamic equation. This is accomplished by eliminating both the cumulus parameterization scheme and the latent heat release due to non-convective precipitation. Thus, this DRY experiment has conditions equivalent to those of the BCD (dry baroclinic) mode in the analytical experiments and contains no CISK mechanism (see Sardie and Warner, 1983 for complete definitions of BCD and BCM).

In the analytical model, storm development due to CISK or stable moist processes can be conveniently isolated because the parameterization of the heating allows a natural means of separation. However, it is not possible to completely eliminate feedback between subvortex-scale latent heating and the vortex-scale circulation in a numerical model. By removing the cumulus parameterization scheme, but allowing non-convective precipitation to occur, one does not eliminate CISK-type feedback. Moisture convergence is still occurring on the scale of the simulated polar low and latent heat is still being released, often on smaller scales. Thus, the CISK mechanism is extant, but because the model cannot resolve true convective scales of motion, the feedback probably occurs on *an incorrect time scale.* Hence, the NCO experiment is also equivalent to the BCM/CISK mode (not the BCM mode) in the analytic study, but the heating profile is characteristic of stable latent heating processes.

Because the Bowen ratio increases from 0.05 near the equator to almost 0.50 at 70° N (Sellers, 1965), the potential role of the surface heat flux in polar-low development should not be underestimated. Økland (1977) has shown using an analytic model that the sensible heat flux from the ocean plays an important role in the development of polar lows. The NFL experiment was designed to evaluate this dependence by removing the parameterizations of the surface sensible and latent heat fluxes.

We do not attempt to use the numerical experiments to clarify the importance of barotropic instability as a development mechanism for these two cases because theoretical arguments are convincing that it cannot represent a significant factor. Specifically, Nitta and Yanai (1969) have presented growth rate curves for easterly and westerly jet maxima for different wavelengths, wind shears and half-widths of jet maxima (Fig. 1, their paper). For this case in the Pacific, a jet maximum of 80 m s^{-1} with a half-width of 5° latitude would produce a growth rate of $\sim 1.6 \times 10^{-6}$ s^{-1}. This very small rate implies that barotropic instability cannot be an important contribution to disturbance growth, even though the necessary condition for barotropic instability is fulfilled. The Atlantic case possesses no shear zones that are barotropically unstable.

5. Discussion of results

Model simulation results are now presented for the two control simulations (Subsection 5.1) and for the three sensitivity experiments (Subsection 5.2). As noted earlier, an interpretation of the results will be provided in Section 6 and a comparison of the analytical and numerical model results in Section 7.

5.1. Discussion of the control experiments

Before any sensitivity studies can be used in verifying hypotheses on polar-low development, it is essential to demonstrate that these polar lows can be modeled successfully. In this section, the CFC and the CAK simulations are compared with the observations, and a discussion of general model performance is provided. This section is divided into two subsections, the first being devoted to the Atlantic case and the second to the Pacific case. In the latter case, the structure of the Gulf of Alaska low is compared with that of the polar low, so that differences and similarities between the two become evident.

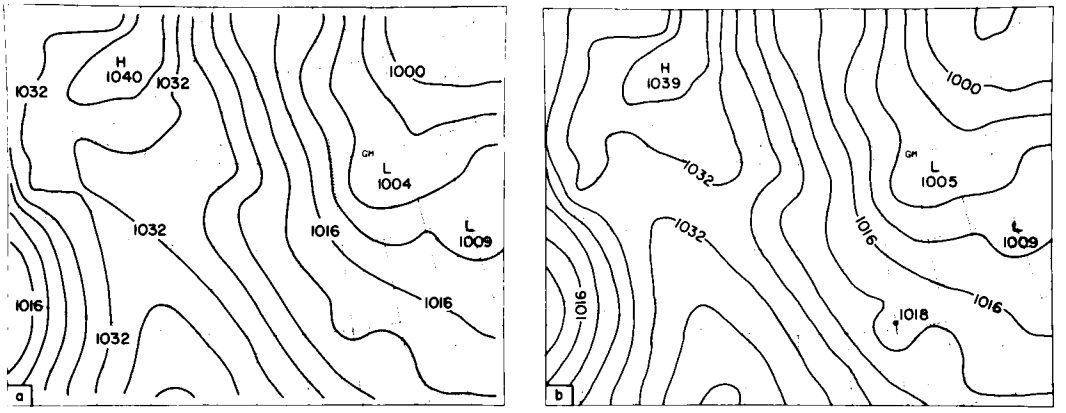

Fig. 6. Forecast MSL pressure (mb) for the Atlantic domain for CFC (a) and CAK (b) at 48 h.

5.1.1. The Atlantic case. The Atlantic CFC experiment was run for 48 h, by which time the polar low was in its mature stage over the Norwegian Sea. The 48-h forecasts of the MSL pressure field for CFC and CAK are shown in Fig. 6. These forecasts should be compared with the analysis of the observations shown in Fig. 2c. In both experiments, the forecast polar low is approximately 5° longitude further northeast than the observed polar low. However, the central pressures of the CFC polar low (1004 mb) and the CAK polar low (1005 mb) compared very well with the observed value (1003 mb). In both forecasts, a low with a central pressure of 1009 mb formed over southern Norway (referred to here as the Norwegian low) and a weak trough developed over the Irish Sea (referred to here as the Irish Sea trough). Note that there is no indication of an Irish Sea trough or a Norwegian low in the analysis of the observations at 48 h (Fig. 2c).

Fig. 7 illustrates the relative vorticity profiles associated with the center of the polar low for the observations, CFC and CAK at 48 h. All three profiles compare favorably, except below 800 mb. Considering that there are no observations over the Norwegian Sea, and that the observed vorticity profile is calculated from NMC's smooth analyses of the winds, the disparity between the observed and the forecast fields is not surprising.

Fig. 8 shows profiles of potential temperature at the core of the polar low at 48 h for the observations, CFC and CAK. These profiles are frequently more informative than cross sections when illustrating conditions in the polar low,

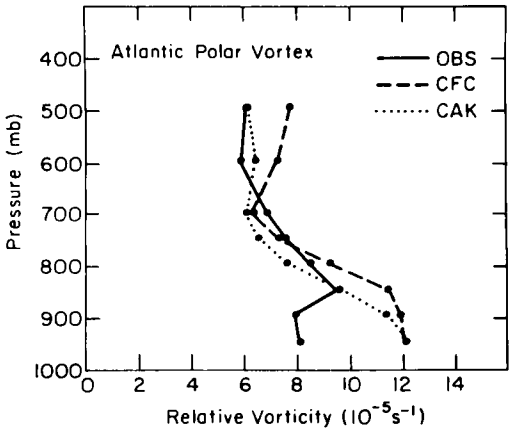

Fig. 7. Vertical profiles of relative vorticity (10^{-5} s^{-1}) at the center of the Atlantic polar low at 48 h, based on observations, CFC and CAK.

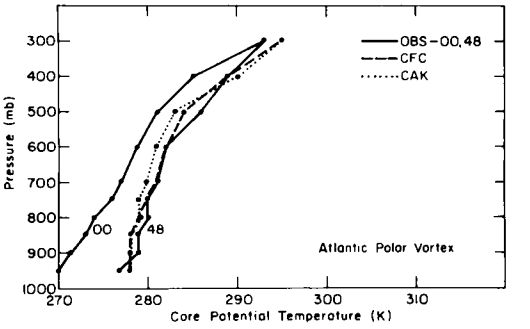

Fig. 8. Vertical profiles of potential temperature (K) at the center of the Atlantic polar low, based on observations at 00 h and 48 h, and CFC and CAK at 48 h.

because they allow for a phase shift of the center of the polar low with height. The forecast potential temperature profile for CFC is in excellent agreement with the observed profile. There is less than one Kelvin degree difference at all levels. The CAK profile is very similar to the CFC profile, except it is slightly cooler in the middle troposphere. This is in agreement with the heating profile differences. The initial observed profile is plotted for reference.

In summary, the model has captured the essential features of the Atlantic polar low. The changes in the central MSL pressure, the 850 mb vorticity maximum and the polar low's thermal structure were all forecast well.

The difference between the results of CFC and CAK are sufficiently small, compared with the differences among the sensitivity experiments described in the next section, to allow us to be confident that the sensitivity results described in the next section are independent of the choice of the convective heating profile.

5.1.2. The Pacific case. The Pacific CFC experiment was run for 36 h, by which time the polar low was in its mature stage and located off the Washington State coast of the US. The smooth NMC analysis (not shown) places the polar low off the Washington coast with a central pressure of 986 mb, while the Locatelli et al. (1982) (hereafter referred to as LOC) analysis of the observations places the polar low further north, with a central pressure of 981 mb (see Figs. 13e and f, their paper). The LOC analysis of the observations will be used for our forecast verification.

Fig. 9 is a graph of the central MSL pressure of the polar and the Gulf lows, plotted as a function of time, as the polar low moved around the Gulf low during the 36-h simulation period. The central pressure of each low, based upon the NMC and LOC analyses of the observations, is shown for reference. The CFC and CAK polar lows deepened only slightly during the first 18 h of the forecast and then deepened rapidly during the last 18 h, consistent with the observations. This compares very favorably with the LOC analysis—a final forecast minimum pressure of 978 mb (CFC) or 979 mb (CAK) compared with a LOC value of 981 mb. The Gulf low deepened to 953 mb and then filled to 965 mb, for both CFC and CAK. This latter value compares very favorably with the NMC analysis of 967 mb for the central pressure of the Gulf low.

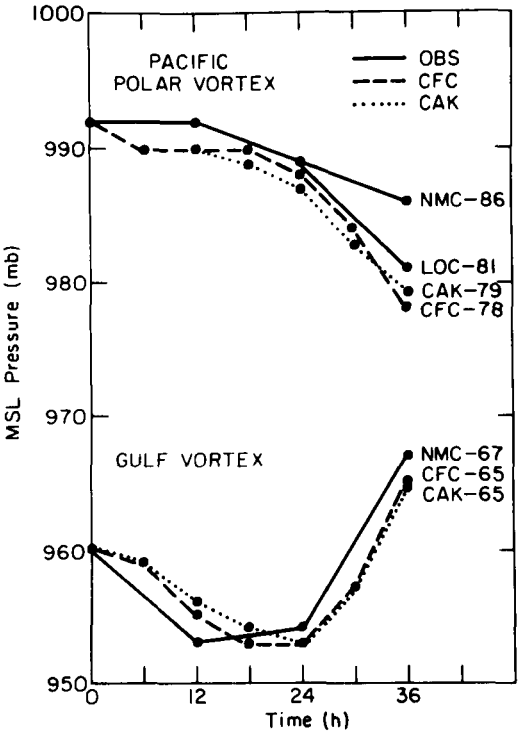

Fig. 9. Central MSL pressure (mb) as a function of time (h) for the Pacific polar low, based on observations, CFC and CAK.

Fig. 10 shows the observed and predicted profiles of the relative vorticity maxima associated with the centers of the polar and Gulf lows at 36 h. The CFC vorticity profile for the polar low approximates the observed profile marginally better than does the CAK vorticity profile. Also, the Gulf low seems to be more insensitive to the vertical heating distribution than does the polar low. Because there are no observations over the Gulf of Alaska and only one radiosonde station on the Alaskan Peninsula, the observed vorticity profiles are based only on a very smooth NMC wind analysis. Thus, the disparity between observed and forecast vorticity profiles should not be surprising.

Fig. 11 shows profiles of potential temperature at the core of the polar and Gulf lows. There is no significant difference between CFC and CAK for the Gulf low and only minor differences for the polar low, where the forecast thermal profiles tend to be colder than observed in the lower troposphere. This may be because the forecast

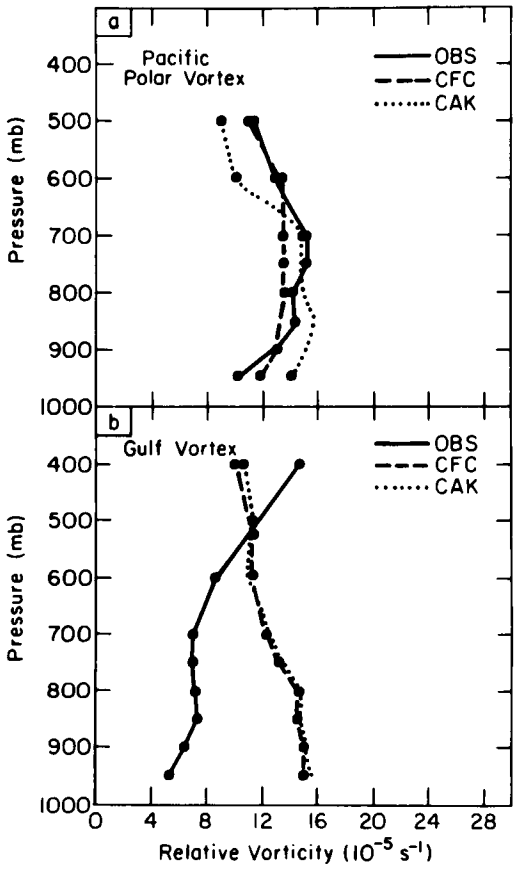

Fig. 10. Vertical profiles of relative vorticity (10^{-5} s $^{-1}$) at the center of the Pacific polar low (a) and the Gulf low (b) at 36 h, based on observations, CFC and CAK.

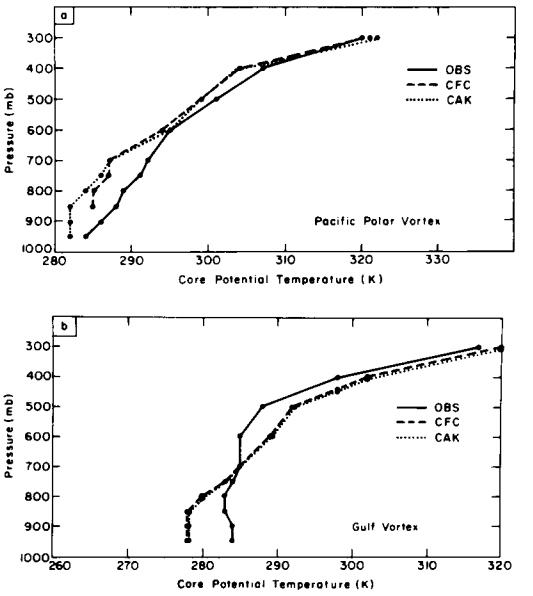

Fig. 11. Vertical profiles of potential temperature (K) at the center of the Pacific polar low (a) and Gulf low (b) at 36 h based on observations, CFC and CAK.

polar low is further north than the observed low. The lack of data may also partially explain the disparity between the observed and forecast profiles. Note that the maximum pressures in the plots of the thermal profiles for the polar low are different for CAK and CFC because a small positional difference in the lows has caused the CFC low to be centered over elevated terrain along the western slope of the Rocky Mountains in the northwest US and one to be located near the coast.

Thus, the model has also captured most of the major features of this developing Pacific polar low. This low originated in a somewhat organized convective cloud cluster in a trough extending southwestward from the Gulf low, and the model developed a well-defined closed-isobar polar low in the correct time period. The movement of the predicted polar low corresponds well with the observations and the major development has been predicted in the last 12 h of the forecast period, consistent with the observations. The vorticity profile (Fig. 10a) of the polar low and its thermal structure (Fig. 11a) are well captured by the model and compare very well with the observations. As in the Atlantic case, the differences between the results of CFC and CAK for the polar low are small compared with the differences between the sensitivity experiments to be discussed in Subsection 5.2.

5.2. *Discussion of the sensitivity experiments*

Having verified that the model is capable of simulating the intensification of the Atlantic polar low and the development of the Pacific polar low from its origins in a small convective cloud field, it is now possible to evaluate the relative importance, to polar-low development, of the different physical mechanisms. This is done by determining how sensitive the model solution is to the removal of the mathematical representation of the various physical processes. In Subsection 5.1, the results of the control experiments were compared with the observations. In this section, the results of the

different sensitivity experiments are compared with those of the CFC simulation. A complete interpretation of the results will appear in Section 6.

5.2.1. The Atlantic case. Fig. 12 shows the forecast MSL pressure fields at 48 h for DRY, NCO and NFL. These fields should be compared with those from CFC and CAK (Fig. 6) and the observations (Fig. 2c). All three sensitivity forecasts show movement of the polar low that is similar to that of the control forecasts. In NCO, three low-pressure centers exist at 48 h; the polar low, a lee low on the eastern side of the Norwegian Mountains and the Norwegian low. Note that the Irish Sea trough and the Norwegian low are only present in NCO and not in NFL or DRY. In general, the results of NFL show the greatest departure from those of CFC. The NFL polar low has a 48-h central MSL pressure of 1009 mb compared with 1004 mb for CFC. The results of NCO show the least departure from those of CFC, the NCO polar low having a 48-h central MSL pressure of 1006 mb, compared with 1004 mb for CFC. The central MSL pressure of DRY is between those of NFL and NCO.

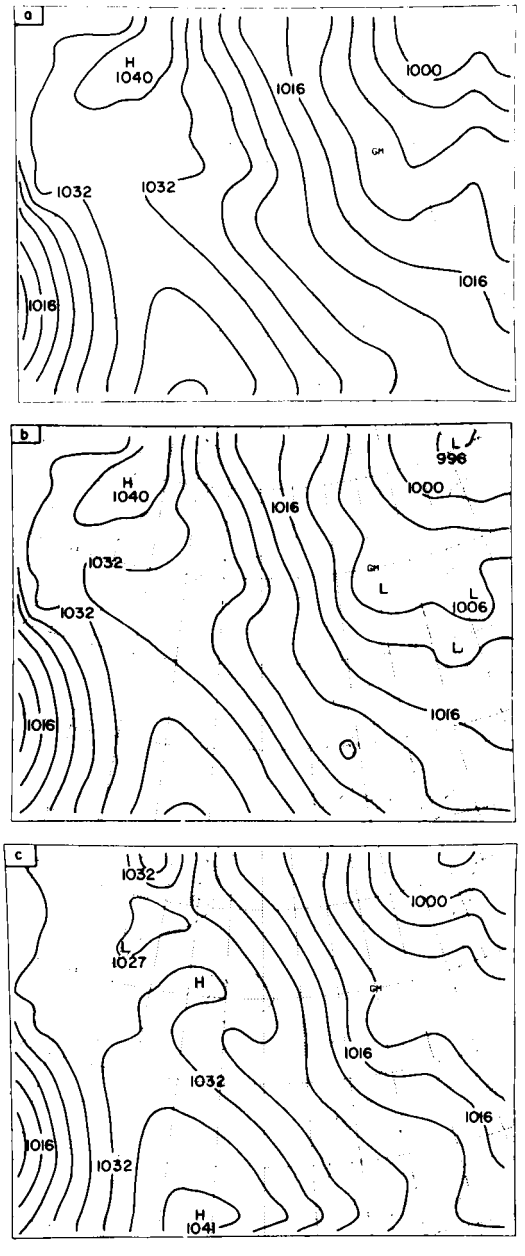

Fig. 12. Forecast MSL pressure (mb) for the Atlantic domain for DRY (a), NCO (b) and NFL (c) at 48 h.

Fig. 13 shows plots of the convective (RC) and non-convective (RNC) rainfall maxima associated with the polar low as a function of time in the three moist experiments. In CFC and NFL, both types of rainfall are reduced to almost zero as the polar low crosses Iceland during the period from 6 h to 12 h. In NCO, the RNC is reduced by more than half during this period. Note that in CFC, RNC is generally slightly larger than RC. When surface heat and moisture fluxes are eliminated (NFL), both RC and RNC are greatly reduced during the last 24 h. In NCO, there is a three-fold increase in RNC during the last 24 h, where there is no trend in the control.

Fig. 14 illustrates the vertical profiles of relative vorticity at 48 h. The results of DRY depart the most from those of CFC. An absence of latent heating reduces the vorticity by half in the lower levels and reduces the height of the top of the polar low from 400 to 600 mb. Surprisingly, lack of surface fluxes weakens the polar low more above 700 mb than below. In NCO, the vorticity profile is similar to that of CFC.

Fig. 15 shows a vertical profile of potential temperature at the core of the polar low at 48 h. This figure should be compared with the observations in Fig. 8. The difference between the controls and the observations is much less than the difference between the controls and the sensitivity experiments. The results of NFL depart the most from those of CFC. The model simulates a steady surface sensible heat flux of ~25 W m^{-2} in the

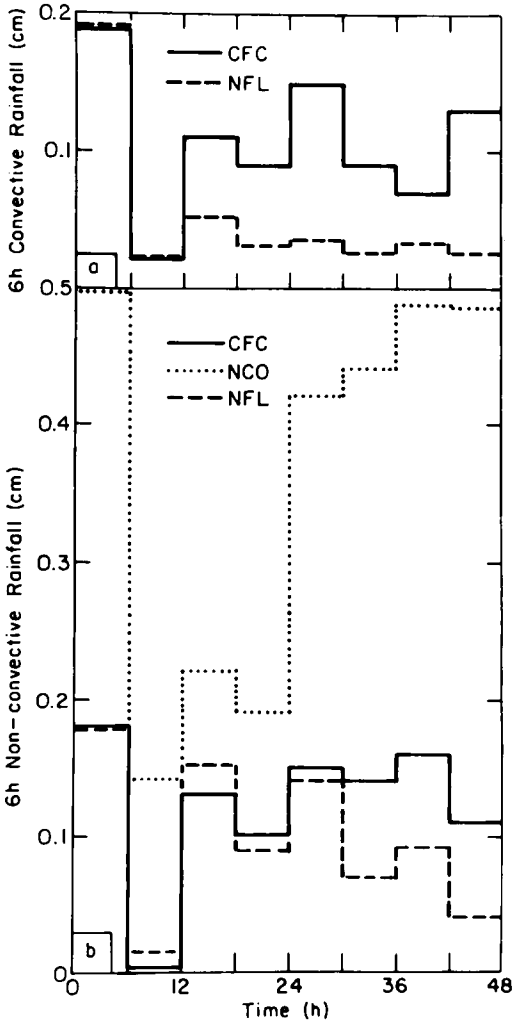

Fig. 13. The 6-hourly convective (a) and non-convective (b) rainfall (cm) as a function time (h). The numbers plotted represent the maxima of the rainfall centers associated with the developing polar low.

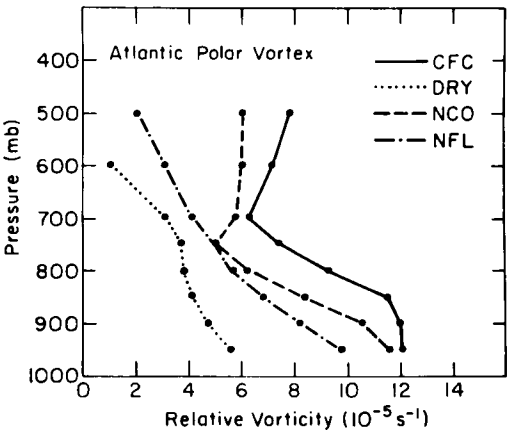

Fig. 14. Vertical profiles of relative vorticity (10^{-5} s^{-1}) at the center of the Atlantic polar low at 48 h for CFC, DRY, NCO and NFL.

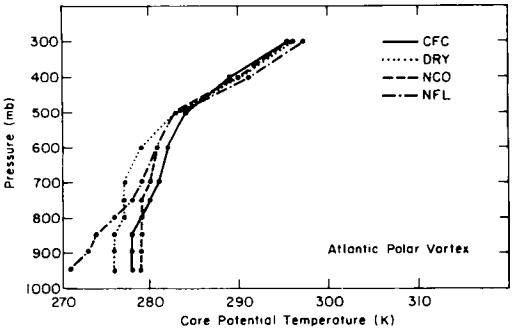

Fig. 15. Vertical profile of potential temperature (K) at the center of the Atlantic polar low at 48 h for CFC, DRY, NCO and NFL.

vicinity of the polar low during the last 30 h of the CFC simulation. Without this heat flux, there is significant cooling in the core of the polar low in the lower layers of the model atmosphere. Indeed, there is as much as 7 K cooling at 950 mb, with some cooling apparent up to 500 mb. The results of DRY also depart significantly from those of CFC. Lack of latent heating has caused at least 2 K lower temperatures at all levels up to 500 mb, with a maximum difference of 4 K between 600 and 700 mb. This is consistent with the Fritsch/Chappell heating profile shown in Fig. 1a. The results of NCO are similar to those of CFC. There is ~1 K positive departure below 800 mb and ~1 K negative depature between 800 and 500 mb.

5.2.2. The Pacific case. Fig. 16 is a graph of the central MSL pressure of the polar and Gulf lows as a function of time, as the polar low moved around the Gulf low during the 36-h simulation period. Note the relative sensitivity of the Gulf and polar lows to the different physical parameterizations, the Gulf low being much less sensitive than the polar low in terms of the final MSL pressure. The results of NFL show the least departure from those of CFC. In DRY, the polar low that is deprived of latent heating does not deepen as much as in CFC.

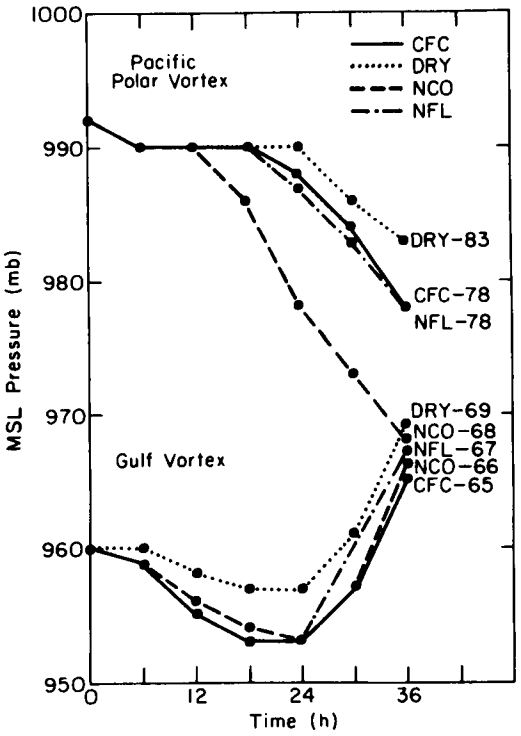

Fig. 16. Central MSL pressure (mb) as a function of time (h) for the Pacific polar low and Gulf lows, based on CFC, DRY, NCO and NFL.

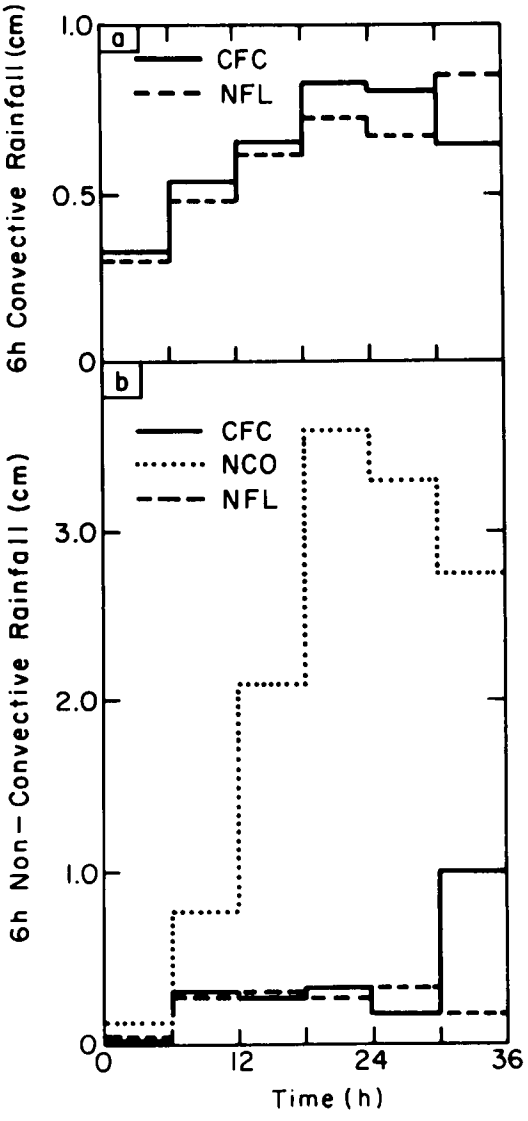

Fig. 17. The 6-hourly convective (a) and non-convective (b) rainfall (cm) as a function of time (h). The numbers plotted represent the maxima of the rainfall centers associated with the developing polar low.

In NCO, the polar low deepens 10 mb more than in CFC.

Fig. 17 shows plots of the convective (RC) and non-convective (RNC) rainfall maxima associated with the polar low as a function of time for the three moist experiments. The CFC convective rainfall plot is not very different from the plot for NFL. The RC in CFC reaches a maximum shortly after 18 h. It is after this time that the major development of the polar low takes place. The RNC for CFC is not too different from NFL, except during the final 6 h. Notice the nine-fold increase in RNC when the convective parameterization is eliminated.

Fig. 18 shows the vertical profiles of relative vorticity at 36 h for the polar and Gulf lows. For the polar low, the vorticity below 800 mb in NCO is more than twice that of the observations and CFC. The vorticity profile for NFL is similar to that of CFC, except below 850 mb. In DRY, the vorticity is larger than in CFC below 850 mb, but less above. For the Gulf low, there is hardly any sensitivity among the results of the different experiments, except for DRY.

Fig. 19 shows a vertical profile of potential temperature at the core of the polar and Gulf lows. With the exception of NFL below 800 mb, the core temperature of the Gulf low is much less sensitive

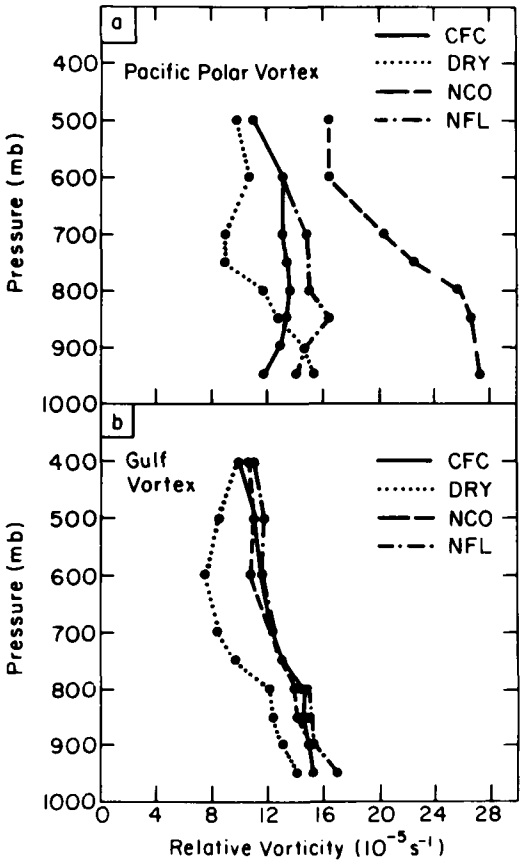

Fig. 18. Vertical profiles of relative vorticity (10^{-5} s^{-1}) at the center of the Pacific polar low (a) and the Gulf low (b) at 36 h for CFC, DRY, NCO and NFL.

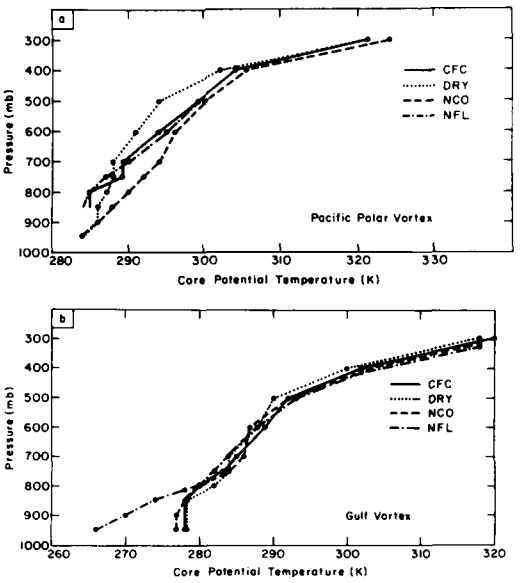

Fig. 19. Vertical profiles of potential temperature (K) at the center of the Pacific polar low (a) and the Pacific Gulf low (b) at 36 h for CFC, DRY, NCO and NFL.

than that of the polar low. For the polar low, the profile of NFL is similar to that of CFC. The profile for NCO is ~5 K warmer at 700 and 800 mb than for CFC, while the profile for DRY is ~5 K cooler at 500 mb than for CFC.

6. Interpretation of the experimental results

6.1. Interpretation of the dynamic processes associated with the CISK mechanism

This subsection is devoted to a discussion of the concept of CISK, with an emphasis on those attributes that are pertinent to the physical interpretation of the results of the numerical experiments discussed in this chapter. Specific factors to be considered involve the nature of the vertical distribution of latent heating associated with CISK and the importance of surface fluxes of sensible and latent heat in the vicinity of the developing vortex.

The vertical distribution of latent heating, both in the atmosphere and the model, depends on the mechanism of precipitation production—either convective or non-convective. It is clear from theoretical considerations and modeling studies that the intensification of a cyclonic circulation is very sensitive to this vertical heating distribution. This is reaffirmed in our earlier sensitivity studies using the analytical model (Sardie and Warner, 1983). These results showed that growth rates of polar lows in a baroclinic atmosphere increase as more latent heat is released lower in the troposphere, for both a convective and a non-convective latent heating parameterization (Fig. 3—Sardie and Warner, 1983). However, growth rates were greater when the same amount of latent heat was released in stratiform cloud (BCM) compared to cumuliform cloud (BCD/CISK). Primitive-equation modeling studies have also demonstrated similar sensitivities. For example, Anthes and Keyser (1979) showed that a low in the Gulf of Mexico deepened by 16 mb more than observed when latent heat was released excessively

low in the troposphere. Also, Anthes et al. (1983) found that the greatest deepening of the Queen Elizabeth II storm was obtained when only non-convective precipitation was allowed, i.e., when using a moisture cycle analogous to the one employed in the NCO experiment.

Let us now review the two conceptual mechanisms of precipitation production/latent heat release for both the atmosphere and a numerical model. On the synoptic scale, condensation occurs when stable lifting produces saturation, for example in the vicinity of a frontal surface or associated with inflow into a developing vortex. In contrast, condensation is also produced in small-scale convective elements that form in a conditionally unstable environment. Latent heating associated with both the stable and unstable processes can affect the intensification of large-scale vortices. The CISK process occurs if the convective condensation becomes sufficiently organized, so that a positive feedback develops between the cloud scale and the developing vortex scale, where the vortex-scale motion provides moisture convergence for the convective process and the cumulus-scale provides the heating that can intensify the large-scale disturbance. Even though the cumulus clouds release latent heat at the levels where condensation occurs, only a small fraction of this heat energy is retained in the convective region—only that necessary for local adjustment of the mass and momentum fields. The rest of the released energy is transmitted by gravity waves to the environment (Ooyama, 1969). The upward motion within the cumulus clouds causes a compensating downward motion, inducing subsidence warming. This causes a heating profile with a level of maximum heating that tends to be in the upper troposphere, as reflected in the Fritsch/Chappell or Anthes heating profiles (Fig. 1). The specific reasons for this are threefold. First, the lower troposphere is generally conditionally unstable, while the upper troposphere is often stable. Thus, subsidence will cause more adiabatic warming in the upper troposphere than in the lower troposphere. Second, the convective eddies transport heat upwards. Third, because of net lateral entrainment into the cloud, the vertical mass flux at any level is greater than at any lower level in a cumulus cloud. Thus, the compensating subsidence at this higher level in the troposphere will induce more warming than at lower levels (J. M. Fritsch, personal communication).

Using the Pacific polar-low case as an example, consider the difference in the forecast polar-low development when only non-convective heating was allowed (NCO) compared to the case where convective and non-convective heating were permitted (CFC). In the NCO experiment, most of the latent heat was released in the 900–700 mb layer of the polar low, as suggested by forecast relative humidity profiles. Latent heat release will cause a mass-field adjustment that induces convergence near the base of the heated region and divergence above it. Thus, warm, moist air from low-levels will be incorporated into the polar low near the base of the heated region. On the other hand, if latent heat is released according to a convective heating profile similar to that of CFC or CAK, most of the latent heat will be released at higher levels, in the 700–500 mb layer (Fig. 1b). Now the latent heat release will cause convergence at mid-tropospheric levels, i.e., ~700 mb. This air is cooler and drier than the air incorporated into the polar low as a result of the non-convective heating. This difference should cause condensation to occur on a faster time scale when non-convective heating at low levels prevails in contrast to higher-level convective or non-convective heating. Thus, it is logical that the NCO polar low should deepen more rapidly than a polar low simulated with a convective heating profile.

We now consider the relationship of surface fluxes of heat and moisture to the rate of development of disturbances. According to Haltiner (1971), when only baroclinic processes exist, growth rates of disturbances are smaller when a sensible heat flux exists at the surface. However, the Atlantic-case results of this study show that the surface sensible and latent heat fluxes were necessary for the correct development of the polar low. Thus, it seems probable that the surface fluxes were related to processes associated with the CISK mechanism in this case. In fact, Økland (1977) has shown with an analytic model that the sensible heat flux from the ocean plays an important role in the development of polar lows when the CISK mechanism is operating. The physical mechanisms responsible for the dependence of growth rates on surface heat and moisture fluxes are examined separately.

An upward surface *moisture flux*, in a region of existing low-level velocity convergence, increases the moisture convergence which causes greater and probably earlier latent heat release which, in turn, causes larger and earlier induced subsidence warm-

ing in the environment of the cumulus clouds. This warming occurs on the vortex scale in the atmosphere and in the model and is what reduces the central MSL pressure of the vortex. This, of course, in turn increases the low-level moisture convergence which maintains the positive feedback. To understand the importance of surface *sensible heat fluxes*, recall that upward motion is proportional to the Laplacian of the local diabatic heating rate. That is, a surface sensible heat flux increases the upward motion within the core of a polar low, if the heat flux pattern has a maximum near the polar low. This increased upward motion within the polar low is associated with an increase in the low-level moisture convergence and thus an increase in the condensation rate. As before, this is responsible for more rapid development of the polar low. In summary, the surface fluxes of both heat and moisture can enhance development of the polar low through the CISK mechanism or its parameterization.

6.2. *The Atlantic case*

Recall that a strong horizontal temperature gradient existed between Greenland and the waters of the Denmark Strait (Fig. 3). This shallow, topographically enhanced baroclinic zone reached the 700 mb level, its intensity being as strong as the deeper, large-scale, frontal baroclinic zone over Great Britain.

The importance of this semipermanent baroclinic zone as a source of available potential energy (APE) for this developing polar low during the first 24 h of its simulation is illustrated here by comparing the observations with DRY and CFC at 24 h and 48 h. We note specifically that the DRY polar low filled 4 mb more during the 48-h simulation than did the observed one, and the relative vorticity profile of the DRY polar low at 48 h showed a significantly weaker structure at all levels than did the profile based on observations or the profile from the control experiments. During the passage of the DRY polar low across Iceland within the first 24 h of the simulation, the central MSL pressure and the low-level vorticity field remained similar to those of the observed polar low. This implies that baroclinity was the dominant mechanism during the first 24 h of the simulation. This is consistent with the fact that the CISK mechanism was not supported by significant surface fluxes of heat and moisture during the period.

The fact that the solution from DRY departed significantly from the observations during the 24–48 h period, implies that moist processes were important for the correct evolution of the polar low during this period. Both the central MSL pressures and the low-level vorticity fields for the CFC and DRY polar lows, which were similar at 24 h, differed sufficiently by 48 h to demonstrate that latent heating played a significant rôle in the intensification of the Atlantic polar low during the last 24 h of the 48-h simulation. The effect of its vertical distribution on the development of the polar low is evaluated by comparing the results of the CFC simulation and the NCO experiment. In NCO, a low-pressure center developed to the lee of the Norwegian mountains. Both the polar and lee lows had a central pressure of 1006 mb. The lee low should not be confused with the Norwegian low over southern Norway. The Norwegian low developed in both the CFC and NCO experiments, while the lee low only developed in the NCO experiment.

Consider the differences in the vertical distribution of latent heating between the CFC simulation and the NCO experiment. Based on forecast relative humidity profiles (not shown), the NCO experiment produced latent heating at lower levels (850–500 mb) than did the CFC experiment (700–500 mb). This is consistent with the 48-h profiles of potential temperature (Fig. 18) for the NCO and CFC polar lows, where the NCO polar low experienced more warming in the 950–800 mb region than did the CFC polar low. Thus, the NCO polar low should deepen more rapidly than the CFC polar low because releasing latent heat lower in the troposphere tends to decrease static stability and enhance development of a vortex, as discussed in the previous subsection. The reason that this did not occur in this case can be seen by comparing the cross sections of forecast potential temperature for the polar low and the lee low in NCO with the cross section of potential temperature for the polar low in CFC (not shown). The lee low in NCO developed a more intense warm-cored structure than did either of the polar lows in NCO and CFC. Because there was only a small upward flux of heat and moisture at the surface over Norway and because the baroclinic zone was closer to the polar low than the lee low in NCO, it seems likely that this more intense warm-cored structure for the lee low existed because of additional latent heat release.

This implies that the lee low obtained a significant fraction of the water vapor that was available through large-scale convergence. Thus, it is likely that the lee low in NCO inhibited the development of its neighboring polar low.

The importance of the surface fluxes of heat and moisture and their relationship to the CISK mechanism is now illustrated by comparing the CFC simulation and the NFL experiments. The NFL polar low filled by 5 mb more than the CFC polar low, and the vorticity at all levels of the NFL polar low exhibits magnitudes that are less than those of the CFC polar low. Based on this evidence it can be concluded that, during the last 24 h of the 48-h simulation, surface fluxes of heat and moisture played an essential role in maintaining the intensity of the polar low. It is especially interesting to note the importance of the surface fluxes on the upper-level development of the polar low. For example, the absence of surface fluxes produced a weakening in the vorticity that was greater above 700 mb than below. The absence of surface fluxes was also noticed in the mass field up to 500 mb. One mechanism by which surface fluxes can affect the mass and wind field of the polar low at upper tropospheric levels is *through the convective feedback of the CISK mechanism*, as discussed in the previous section. Support for the importance of this mechanism is provided by comparing the convective rainfall fields in NFL and CFC (Fig. 13a). Specifically, when no surface fluxes existed, the convective rainfall was decreased by a factor of two.

6.3. *The Pacific case*

The Pacific polar low developed in a stronger and deeper baroclinic zone than did its Atlantic counterpart. The importance of this baroclinic zone as a source of available potential energy for the polar low is illustrated by comparing the observations with the results of the DRY experiment. In terms of the surface development, this polar low intensified from its genesis as a small convective cloud field, by 9 mb out of the observed 11 mb, through dry baroclinic processes alone. However, upper-level features of the polar low were not reproduced well by baroclinic processes alone.

The effects of latent heat release on development are further revealed through a comparison of the results of the DRY experiment and the CFC simulation. The polar low in CFC deepened by 5 mb more than the one in DRY. Although the Pacific polar low intensified by 9 mb through baroclinity alone, latent heating was essential to obtain the *correct* deepening rate. Latent heating was also necessary to obtain the observed thermal and vorticity profiles. The sensitivity of the development of the polar low to the vertical distribution of the latent heating is evaluated by comparing the results of the CFC simulation and the NCO experiment. The NCO polar low deepened by 10 mb more than the one in CFC. Based on forecast relative humidity profiles (not shown), it can be seen that most of the latent heat was released in the 1000–700 mb layer in NCO, while the latent heat release extended through the 1000–500 mb layer in CFC. As discussed in Subsection 6.1, the release of latent heat lower in the troposphere causes more rapid development of a vortex. In NCO, the fact that the latent heat release was limited to the lower troposphere, caused development on a shorter time scale and increased the low-level vorticity by more than a factor of two compared with the value in CFC. Thus, convective as well as the non-convective latent heating were essential for the observed development of the Pacific polar low.

The importance of surface fluxes of heat and moisture to the developmemt of this polar low is illustrated by comparing the results of the CFC simulation and the NFL experiment. The central MSL pressure of the NFL polar low has the same value as that of the CFC polar low, and both the convective and non-convective rainfall amounts of NFL were similar to those of CFC. Even though both the Atlantic and Pacific polar lows received steady, average surface heat fluxes of ~ 25 W m^{-2}, only in the Atlantic case did surface fluxes contribute to the intensification of the polar low. The path of the Pacific polar low roughly followed the predicted zero heat-flux isopleth, and consequently it never experienced a maximum in the heat flux field. On the other hand, the Atlantic polar low traversed a heat flux maximum over the Norwegian Sea during the last 24 h of the 48-h simulation. Thus, surfaces fluxes had little effect on the development of this polar low.

It is worth noting that *non-convective* precipitation dominated in the vicinity of the Gulf low during the 48-h period. Thus, it is not surprising that the results of NCO are very similar to those of CFC for the Gulf low.

7. Comparison of analytical and numerical model results

The analytical experiments and their associated sensitivity studies are discussed in Sardie and Warner (1983). The results are briefly summarized here. The analytic results showed that CISK alone was not sufficient for the genesis of either Atlantic or Pacific polar lows for the seven case studies chosen. Simulated growth rates were just too small. On the other hand, dry baroclinity (BCD mode) was also not sufficient to give either correct length scales or growth rates for both Atlantic and Pacific polar lows. In the combined BCD/CISK mode, observed and predicted growth rates were comparable for Atlantic and Pacific polar lows, but wavelengths were too large in general. In the moist baroclinic-CISK mode (BCM/CISK), where latent heat is released by both convective and stratiform clouds, growth rates and wavelengths predicted by the analytical model were comparable to observed values for the Atlantic cases. They were less comparable but still similar for the Pacific cases. However, model equations became invalid in some cases for the BCM/CISK mode and in all cases for the BCM mode when the moist static stability parameter became negative. In the analytic study of Atlantic polar lows, vertical wind shear that was specified based on observations from the individual case studies, reflected baroclinity that was restricted to the low levels. Thus, an upper-level source of APE resulting from CISK, complemented a lower-level source of APE resulting from shallow baroclinity. Moist baroclinity and CISK were both necessary for observed polar-low development in the Atlantic Ocean. For Pacific polar lows, the observed baroclinic zones were generally deep and intense as reflected in the observations of Mullen (1979) and Reed (1979). Thus, moist baroclinity provided a source of APE throughout the entire troposphere. However, the analytical model did not show that the BCM mode alone was the most likely mode for Pacific polar-low development. Rather, wavelengths and growth rates resulting from the BCM/CISK mechanism were more realistic. When Lau's (1978) climatological data were used in the analytical model, the model predicted the preferred geographic regions where polar lows developed, both in the Atlantic and the Pacific oceans.

The numerical results generally support these conclusions and provide additional insight into the important dynamical processes of polar-low development. The Atlantic polar low experienced a shallow but intense baroclinic zone over the Denmark Strait region during the first 24 h of the forecast. Sensitivity studies revealed that, even though baroclinity was sufficient to allow realistic development while the polar low was in the vicinity of this baroclinic zone, both convective and non-convective latent heating and surface fluxes of sensible heat and moisture, i.e. CISK, were required for observed development after the polar low departed from this baroclinic zone and entered the Norwegian Sea. The convective latent heating profile was essential for the Atlantic polar low to maintain the observed structure and to intensify realistically. A distribution of non-convective latent heating was not sufficient. The fact that convective and non-convective latent heating were essential is consistent with the analytic results.

The Pacific polar low developed in a deep strong baroclinic zone. Consequently, baroclinity was potentially more important in the development of the Pacific polar low than the Atlantic polar low. However, as shown by the evoluation of the central MSL pressure and thermal structure of the polar low, latent heating also played an important role. As demonstrated by the results of the sensitivity experiments, latent heating from both the CISK and the non-convective heating profiles was essential for the observed development of the polar low, even though the polar low developed and moved within this deep, strong baroclinic zone. These results are also consistent with the analytical model results.

8. Acknowledgments

We would like to thank J. Michael Fritsch and William M. Frank for many fruitful and helpful discussions of convection and CISK and also Gregory S. Forbes for his stimulating discussions of the observational evidence of Atlantic polar lows. This research was financially supported by the US Navy under Navy Contract N000014-78-C0775. Computing support was provided by the National Center for Atmospheric Research which is funded by the US National Science Foundation. Lastly, a special thanks is due to Carmel Aiello, and Michele Shawver and Nancy Warner who patiently typed this manuscript.

REFERENCES

Anthes, R. A. 1977. A cumulus parameterization scheme utilizing a one-dimensional cloud model. *Mon. Wea. Rev. 105*, 270–286.

Anthes, R. A. and Keyser, D. 1979. Tests of a fine-mesh model over Europe and the United States. *Mon. Wea. Rev. 107*, 963–984.

Anthes, R. A. and Warner, T. T. 1978. Development of numerical simulations of a case of explosive marine cyclogenesis. *Mon. Wea. Rev. 111*, 1174–1188.

Anthes, R. A. and Warner, T. T. 1978. Development of hydrodynamic models suitable for air pollution and other mesometeorological studies. *Mon. Wea. Rev. 106*, 1045–1078.

Benjamin, S. G. and Seaman, N. L. 1985. A simple scheme for improved objective analysis in curved flow. *Mon. Wea. Rev. 113*, 1184–1198.

Charney, J. G. and Eliassen, A. 1964. On the growth of the hurricane depression. *J. Atmos. Sci. 21*, 68–75.

Duncan, C. N. 1977. A numerical investigation of polar lows. *Q. J. R. Meteorol. Soc. 103*, 255–268.

Forbes, G. A. and Lottes, W. D. 1982. Characteristics and evolution of mesoscale cloud vortices occurring in polar airstreams. *Preprints, Conf. Cloud Physics, Chicago*, Amer. Meteor. Soc., 310–313.

Fritsch, J. M. and Chappell, C. F. 1980. Numerical prediction of convectively driven mesoscale pressure systems. Part I. *J. Atmos. Sci. 37*, 1722–1733.

Haltiner, G. J. 1971. *Numerical weather prediction.* John Wiley and Sons, 1st edition, 317 pp.

Haltiner, G. J. and Williams, R. T. 1980. *Numerical prediction and dynamic meteorology.* John Wiley and Sons, 2nd edition, 477 pp.

Harrold, T. W. and Browning, K. A. 1969. The polar low as a baroclinic disturbance. *Q. J. R. Meteorol. Soc. 95*, 710–723.

Kessler, E. III. 1965. Microphysical parameters in relation to tropical cloud and precipitation distributions and their modifications. *Geofis. Int. 5*, 79–88.

Kuo, H. L. 1965. On formation and intensification of tropical cyclones through latent heat release by cumulus convection. *J. Atmos. Sci. 22*, 40–63.

Kuo, H. L. 1971. A theory of parameterization of cumulus convection. *J. Meteorol. Soc. Japan 49*, 744–756.

Kuo, H. L. 1974. Further studies of the parameterization of the influence of cumulus convention on large-scale flow. *J. Atmos. Sci. 31*, 1232–1240.

Lau, N. 1978. On the three-dimensional structure of the observed transient eddy statistics of the Northern Hemisphere wintertime circulation. *Mon. Wea. Rev. 35*, 1900–1923.

Locatelli, J. D., Hobbs, P. V. and Werth, J. A. 1982. Mesoscale structure of vortices in polar air streams. *Mon. Wea. Rev. 110*, 1417–1433.

Mansfield, D. A. 1974. Polar lows: the development of baroclinic disturbances in cold air outbreaks. *Q. J. R. Meteorol. Soc. 100*, 541–544.

Mullen, S. L. 1979. An investigation of small-scale cyclones in polar air streams. *Mon. Wea. Rev. 107*, 1636–1647.

Nitta, T. and Yanai, M. 1969. A note on the barotropic instability of the tropical easterly current. *J. Meteorol. Soc. Japan 47*, 127–130.

Økland, H. 1977. On the intensification of small-scale cyclones formed in very cold air masses heated by the ocean. *Institute Report Series No. 26*, Department of Geophysics, University of Oslo, Norway.

Ooyama, K. 1969. Numerical simulation of the life cycle of tropical cyclones. *J. Atmos. Sci. 26*, 3–40.

Ooyama, K. 1982. Conceptual evolution of the theory and modeling of the tropical cyclone. *J. Meteorol. Soc. Japan 60*, 369–379.

Rasmussen, E. 1977. The polar low as a CISK-phenomenon. Report No. 6, Department of Theoretical Meteorology, University of Copenhagen, 76 pp. (Available from NOAA, Library and Information Services Division, Rockville, MD 20023).

Rasmussen, E. 1979. The polar low as an extratropical CISK-disturbance. *Q. J. R. Meteorol. Soc. 105*, 531–549.

Rasmussen, E. 1981. An investigation of a polar low with a spiral cloud structure. *J. Atmos. Sci. 38*, 1785–1792.

Reed, R. J. 1979. Cyclogenesis in polar air streams. *Mon. Wea. Rev. 107*, 38–52.

Sardie, J. M. and Warner, T. T. 1983. On the mechanism for the development of polar lows. *J. Atmos. Sci. 40*, 869–881.

Sellers, W. D. 1965. *Physical climatology.* Chicago: University of Chicago, 272 pp.

Zhang, D. and Anthes, R. A. 1982. A high-resolution model of the planetary boundary layer-sensitivity tests and comparisons with SESAME-79 data. *J. Appl. Meteorol. 21*, 1594–1609.